

## 17. STABLE ISOTOPE STRATIGRAPHY AND CHRONOLOGY OF THE UPPER QUATERNARY SECTION AT SITE 883, DETROIT SEAMOUNT<sup>1</sup>

L.D. Keigwin<sup>2</sup>

### ABSTRACT

Stable isotope studies provide a preliminary stratigraphic and chronologic framework for the upper Quaternary section of Ocean Drilling Program Site 883 (Detroit Seamount, far northwest Pacific). Using shipboard magnetic susceptibility results, all four holes at this site were correlated and samples were taken to create a composite sequence for the upper 30 m of the sediment column. Although foraminifers are often completely absent, the benthic genus *Uvigerina* was sufficiently abundant near glacial terminations to identify most oxygen isotope stage boundaries. However, minimum  $\delta^{18}\text{O}$  may not be recorded during full interglacial conditions. Highest resolution chronostratigraphy will probably be achieved through a combination of stable isotope stratigraphy and biostratigraphic techniques. Oxygen isotope results support continuous sedimentation during the past 0.5 m.y. with an average rate of 50 m/m.y.

### INTRODUCTION

One of the main purposes of coring sediments on Detroit Seamount during Ocean Drilling Program (ODP) Leg 145 was to recover sequences suitable for continuous high-resolution paleoclimate studies. From previous work in the far northwest Pacific, it was already known that the sediments blanketing the northern Emperor Seamounts often contain carbonate microfossils and that the sediments accumulate rapidly enough to study paleoenvironmental changes on orbital and shorter time scales (Keigwin, 1987; Keigwin et al., 1992). We cored Site 883 in relatively shallow water (~2400 m) to maximize preservation of foraminifers, and deep Site 884 (~3900 m) to evaluate the paleocirculation significance of the Meiji Drift. Together with intermediate depth Site 882 (~3300 m), the sites form a transect for the reconstruction of depth-dependent sediment fluxes.

Critical to Leg 145 objectives is establishing a detailed chronostratigraphy for the recovered sections. High-resolution correlations between cores may be constructed using GRAPE data and magnetic susceptibility, but late Quaternary chronology at our sites must rest on biostratigraphy or stable isotope stratigraphy. In this report, I discuss a preliminary oxygen isotope stratigraphy for the upper 30 m of the four holes cored at Site 883.

### METHODS

The upper 40 m of the Site 883 holes were correlated using shipboard magnetic susceptibility results to identify missing sediment at core breaks (Fig. 1). These results were found to be consistent with missing intervals identified using gamma-ray attenuation porosity evaluator (GRAPE) data, which was used for tying the Core 1H/2H break at Hole 883D to Hole 883C. A composite sequence was constructed for Site 883 (Table 1), and 10 cm<sup>3</sup> samples were obtained about every 10 cm, avoiding obviously disturbed intervals and ash layers.

Samples were dried, weighed, and washed on a 63 µm screen. The coarse fraction was dried and sieved again at 150 µm; all of the benthic foraminifers *Cibicidoides* and *Uvigerina* were then removed and counted. Many of the results presented here were based on analyses of single specimens because that is all that was available. If necessary, specimens for isotopic analysis were cleaned ultrasonically. Clean specimens of the hispid variety of *Uvigerina* were selected for stable isotope analysis on either a hybrid, computer-controlled, triple collector VG mass spectrometer (following extraction in a common acid bath) or on a Finnigan MAT 252 mass spectrometer fitted with a "Kiel device." Most analyses from Holes 883C and 883D were done on the VG mass spectrometer, and results between the two instruments are compatible without corrections. Where possible, outlying results were replicated; however, four analyses were summarily rejected because they were obvious outliers and there were too few foraminifers for repeat analyses.

### RESULTS AND DISCUSSION

#### Stratigraphy

Oxygen isotope results from the Site 883 composite section show a sequence of oscillations ranging between values of 3.0‰ and 5.0‰, which must reflect the effect of late Quaternary glaciations on the chemical and physical properties of deep waters overlying Detroit Seamount (Fig. 2A and Appendix). Many gaps exist in the record because of the low abundance or complete absence of foraminifers in some intervals (Fig. 2C), but it is clear as noted for the most recent deglaciation on nearby Meiji Seamount (Keigwin et al., 1992), that foraminifers are abundant enough at glacial terminations to establish a crude  $\delta^{18}\text{O}$  stratigraphy. As a check, *Uvigerina* results from Site 883 were compared with those from east equatorial Pacific Site 677 (Shackleton et al., 1990). The principal isotope stages are recognizable back to Stage 14 at Site 883, and the glacial to interglacial changes ("terminations") have been marked by dashed lines (Fig. 2A).

Carbon isotope results also show glacial-interglacial variability with the typical ~0.5‰ range (Fig. 2B), which is thought to reflect the secular change in ocean composition caused by terrestrial biomass decrease during glaciation (Shackleton, 1977; Curry et al., 1988). Although there is some concern about so-called "vital effects"

<sup>1</sup>Rea, D.K., Basov, I.A., Scholl, D.W., and Allan, J.F. (Eds.), 1995. *Proc. ODP, Sci. Results*, 145: College Station, TX (Ocean Drilling Program).

<sup>2</sup>Woods Hole Oceanographic Institution, Woods Hole, MA 02543, U.S.A.

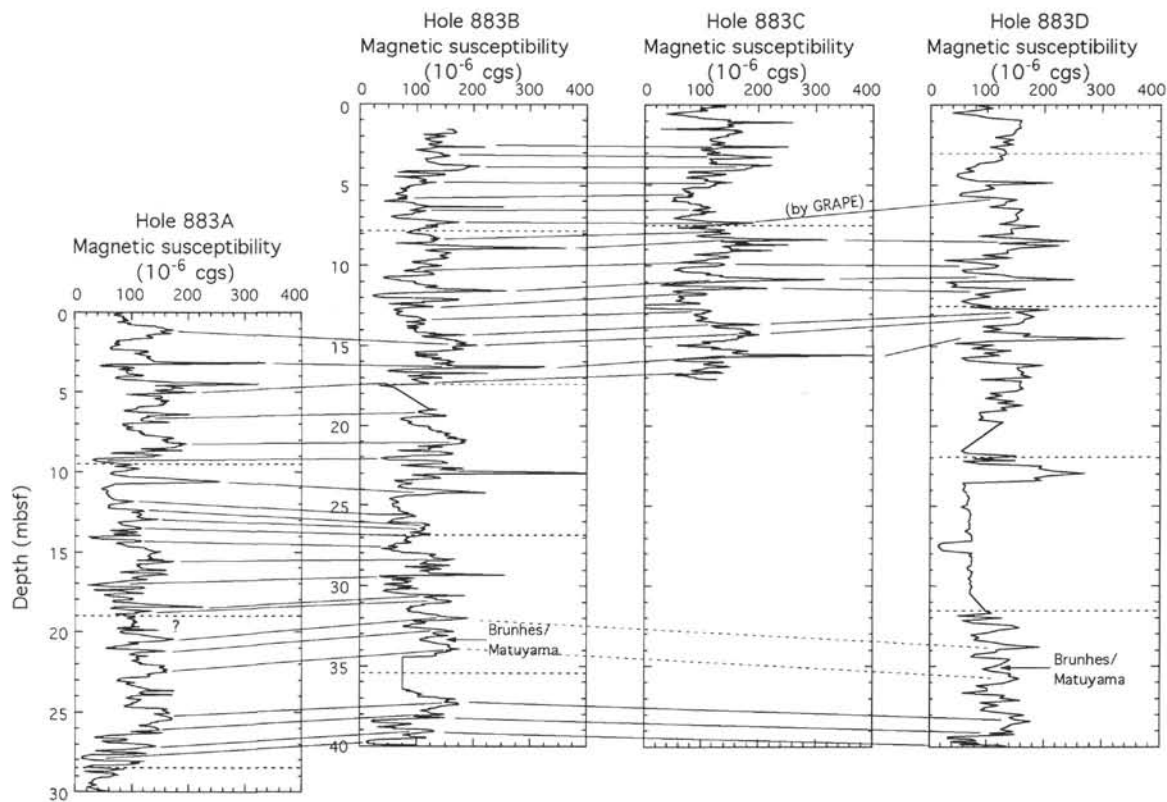


Figure 1. Correlation of the four Site 883 holes using shipboard magnetic susceptibility measurements and GRAPE at one level in Holes 883C and 883D. In addition, the level of the Brunhes/Matuyama boundary is noted in Holes 883B and 883C (Weeks, this volume).

**Table 1. Site 883 intervals used to build a composite section.**

Core, section, interval (cm)	Depth (mbsf)	Composite
145-		
883D-1H-1, 0, to 883D-1H-5, 140	0.00–7.40	0.00–7.40
883C-2H-2, 134, to 883C-2H-3, 145	5.85–7.45	7.40–9.00
883D-2H-1, 0, to 883D-2H-7, 62	7.50–17.18	9.00–18.68
883A-1H-3, 103, to 883A-1H-7, 30	4.03–9.30	18.68–23.95
883B-3H-4, 0, to 883B-3H-7, 61	21.90–27.01	23.95–29.06

on *Uvigerina*  $\delta^{13}\text{C}$  during late Quaternary climate cycles (Zahn et al., 1986) and particularly on deglaciation in the northwest Pacific (Keigwin et al., 1992), at Site 883 *Uvigerina*  $\delta^{13}\text{C}$  consistently increases across the dashed lines marking glacial terminations (except the most recent, in which Stage 1 is not well represented). In other respects, these data are similar to those from elsewhere. For example, benthic foraminiferal carbonate is especially enriched in  $^{13}\text{C}$  in Stage 13, as at Site 677 and northeast Atlantic Site 552 (Raymo et al., 1990). Thus, *Uvigerina*  $\delta^{13}\text{C}$  from Site 883 may prove useful for paleocirculation and paleoclimate studies; however analyses must first be completed on *Cibicidoides* data, which are probably less subject to “vital effects” and which have been calibrated to water-column  $\delta^{13}\text{C}$  at the Detroit Seamount (McCorkle and Keigwin, 1994).

### Chronology

*Uvigerina*  $\delta^{18}\text{O}$  is plotted vs. age together with *Uvigerina*  $\delta^{18}\text{O}$  from Site 677 (Fig. 3) using the new astronomical calibration of Shackleton et al. (1990). This calibration differs from previous late Pleistocene time scales (such as SPECMAP) in that it incorporates an age of 0.78 m.y. for the Brunhes/Matuyama boundary and it is based on orbital tuning. Because I am unaware of any tabulation of revised

ages for this new stable isotope chronostratigraphy, the ages of the distinctive glacial terminations at Site 883 (Fig. 2A) were estimated using Shackleton’s Site 677 data (summarized in Table 2). This age model results in a nearly linear age-depth relationship for Site 883, with a sedimentation rate of  $\sim 50$  m/m.y. (Fig. 4). Even though the data sets from Sites 883 and 677 are forced to correlate at the major terminations in Figure 3, the two records are sufficiently alike that there should be no question about the isotope stratigraphy on the 0.1-m.y. scale. This preliminary chronology is further supported by a stratigraphy based on the abundance of the radiolarian *Cycladophora davisiana* and the last occurrence ( $\sim 0.35$  m.y.) of the radiolarian *Druppatractus acqulonius* (Morley, this volume), as well as the last occurrence ( $\sim 0.30$  m.y.) of the diatom *Simonsenella curvirostris* (Barron, this volume). These two datum levels closely bracket the Stage 9/10 deglaciation at Site 883 (Fig. 3).

### SUMMARY

Benthic foraminifers are not present continuously down Site 883 at  $\sim 2400$  m on Detroit Seamount, but their abundance is sufficient during glacial intervals and on glacial terminations to develop a preliminary isotope stratigraphy and chronology. There is clearly some scope for additional refinement. For example, interglacial Stage 13 seems about 0.015 m.y. too long; however, with the absence of sufficient foraminifers for analysis or reanalysis in critical intervals like Stages 5, 7, 9, or 11, the prospects are not good for a higher resolution  $\delta^{18}\text{O}$  chronostratigraphy through “tuning” the Site 883 record to other sites. Further development of the late Quaternary time scale for the far northwest Pacific can best be made through the correlation of the new  $\delta^{18}\text{O}$  results for Site 883 to high-resolution abundance records of *C. davisiana*, which is abundant during both interglacial and glacial conditions in this region.

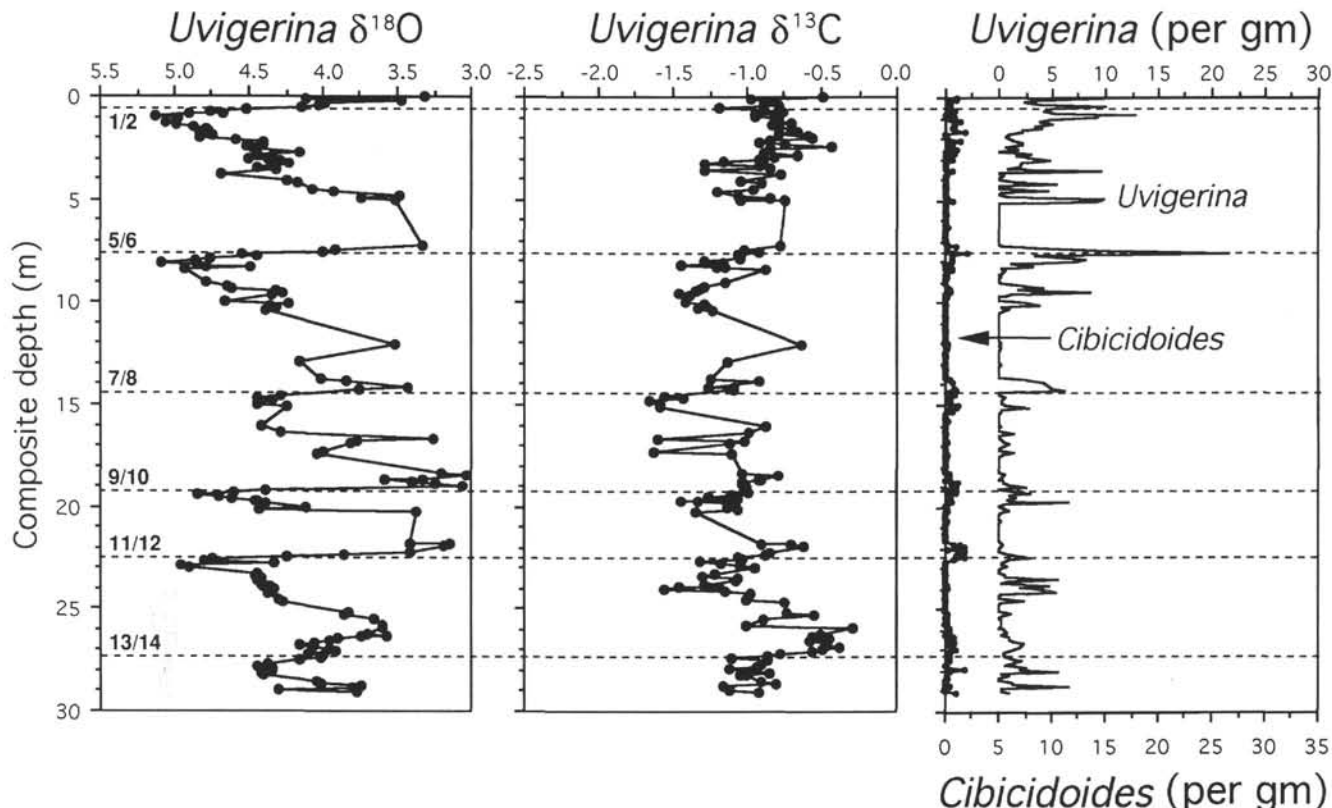


Figure 2. Stable isotope results and abundance results on benthic foraminifers from Site 883 as a function of composite depth (determined according to Fig. 1 and Table 1). Oxygen isotope results on *Uvigerina* show the familiar glacial-interglacial oscillations, with the major glacial to deglacial transitions ("terminations") marked by stage numbers and dashed lines that extend across the figure. Carbon isotope results on *Uvigerina* appear to show the expected secular changes in seawater chemistry, with lower  $\delta^{13}\text{C}$  during glacial intervals; this needs to be verified with analyses on specimens of *Cibicidoides* (see text), which are much less common than *Uvigerina*.

## ACKNOWLEDGMENTS

I thank USSAC for funding this research, Ellen Roosen for washing the samples and picking the foraminifers, C. Eben Franks for making the stable isotope measurements, and Dave Anderson and Bobby C. Thunell for helpful comments on the manuscript.

## REFERENCES\*

- Curry, W.B., Duplessy, J.C., Labeyrie, L.D., and Shackleton, N.J., 1988. Changes in the distribution of  $\delta^{13}\text{C}$  of deep water  $\Sigma\text{CO}_2$  between the last glacial and the Holocene. *Paleoceanography*, 3:317–341.  
 Keigwin, L.D., 1987. North Pacific deep water formation during the latest glaciation. *Nature*, 330:362–364.  
 Keigwin, L.D., Jones, G.A., and Froelich, P.N., 1992. A 15,000-year paleoenvironmental record from Meiji seamount, far northwestern Pacific. *Earth Planet. Sci. Lett.*, 111:425–440.  
 McCorkle, D.C., and Keigwin, L.D., 1994. Depth profiles of  $\delta^{13}\text{C}$  in bottom water and core top *C. wuellerstorfi* on the Ontong Java Plateau and Emperor Seamounts. *Paleoceanography*, 9:197–208.

Raymo, M.E., Ruddiman, W.F., Shackleton, N.J., and Oppo, D.W., 1990. Evolution of Atlantic-Pacific  $\delta^{13}\text{C}$  gradients over the last 2.5 m.y. *Earth Planet. Sci. Lett.*, 97:353–368.

Shackleton, N.J., 1977. Carbon-13 in *Uvigerina*: tropical rainforest history and the equatorial Pacific carbonate dissolution cycles. In Andersen, N.R., and Malahoff, A. (Eds.), *The Fate of Fossil Fuel CO<sub>2</sub> in the Oceans*: New York (Plenum), 401–427.

Shackleton, N.J., Berger, A., and Peltier, W.R., 1990. An alternative astronomical calibration of the lower Pleistocene timescale based on ODP Site 677. *Trans. R. Soc. Edinburgh: Earth Sci.*, 81:251–261.

Zahn, R., Winn, K., and Sarnthein, M., 1986. Benthic foraminiferal  $\delta^{13}\text{C}$  and accumulation rates of organic carbon: *Uvigerina peregrina* group and *Cibicidoides wuellerstorfi*. *Paleoceanography*, 1:27–42.

\*Abbreviations for names of organizations and publications in ODP reference lists follow the style given in Chemical Abstracts Service Source Index (published by American Chemical Society).

Date of initial receipt: 5 April 1994

Date of acceptance: 22 September 1994

Ms 145SR-116

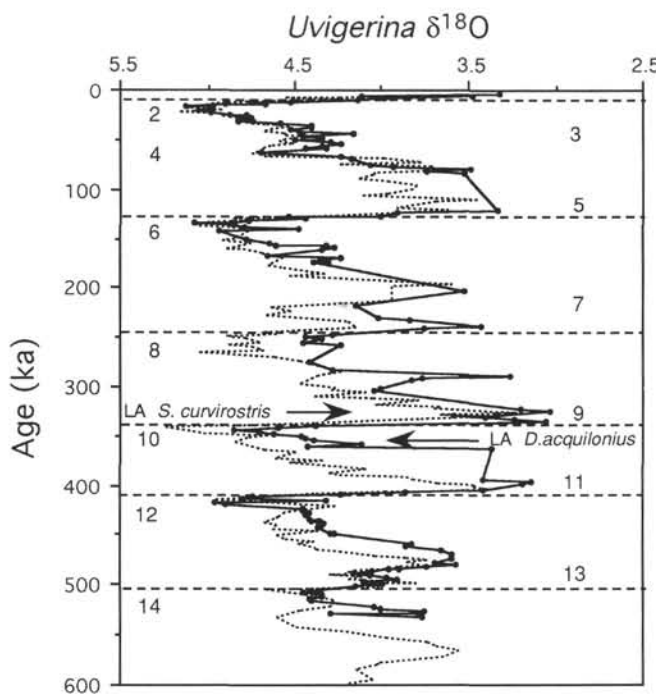


Figure 3. Oxygen isotope results on *Uvigerina* from Site 883 (Detroit Seamount, solid points) and ODP Site 677 (eastern equatorial Pacific, dotted line) plotted on the time scale of Shackleton et al. (1990). Numbers refer to oxygen isotope stages. The last appearances (LA) of *S. curvirostris* and *D. aquilonius* are consistent with the isotope stratigraphy (see text).

Table 2. Age model for Site 883 composite section.

Composite depth (m)	Age (ka)	Comments
0.01	5	Assumed
1.14	18	Assumed
7.56	127	Stage 5/6
14.40	243	Stage 7/8
19.06	336.8	Stage 9/10
22.42	408.3	Stage 11/12
27.56	504	Stage 13/14
41.00	780	Brunhes/Matuyama boundary

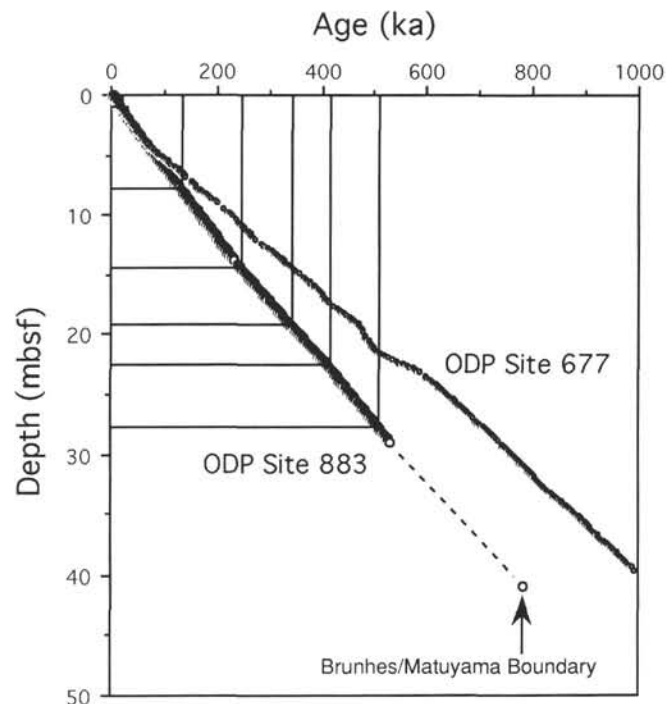


Figure 4. Age-depth relationships for Sites 883 and 677. The chronology for Site 883 is based on comparison to glacial terminations at Site 677, with control points for Site 883 indicated by intersecting lines. Evidently, a nearly constant sedimentation rate of ~50 m/m.y. continues at least to the Brunhes/Matuyama boundary (end of dashed line), at ~41 composite mbsf.

**APPENDIX**  
**Benthic Stable Isotope Data and Foraminiferal Abundance, Site 883**

Core, section, interval (cm)	Depth (mbsf)	Composite depth (m)	$\delta^{13}\text{C}$ <i>Uvig.</i>	$\delta^{18}\text{O}$ <i>Uvig.</i>	Cibs. (N)	<i>Uvig.</i> (N)	Cibs. (per gm)	<i>Uvig.</i> (per gm)
<b>145-883A-</b>								
1H-3, 103	4.04	18.69	-0.91	3.58	3	3	0.45	0.45
1H-3, 112	4.13	18.78	-1.03	3.40	9	3	1.24	0.41
1H-3, 120	4.21	18.86	-1.03	3.24	5	9	0.61	1.1
1H-3, 130	4.31	18.96	-1.01	3.06	10	26	0.99	2.58
1H-3, 140	4.41	19.06			0	0	0	0
1H-4, 0	4.51	19.16	-1.02	4.39	3	10	0.37	1.23
1H-4, 10	4.61	19.26	-0.98	4.60	10	28	1.07	2.99
1H-4, 20	4.71	19.36	-1.10	4.85	4	9	0.44	1
1H-4, 30	4.81	19.46	-1.25	4.70	3	13	0.39	1.69
1H-4, 42	4.93	19.58	-1.05	4.62	3	7	0.33	0.77
1H-4, 51	5.02	19.67	-1.45	4.46	1	14	0.11	1.59
1H-4, 60	5.11	19.76	-1.32	4.44	4	47	0.56	6.57
1H-4, 70	5.21	19.86	-1.11	4.39	1	6	0.11	0.64
1H-4, 81	5.31	19.96			0	0	0	0
1H-4, 92	5.43	20.08	-1.13	4.11	2	4	0.19	0.38
1H-4, 100	5.51	20.16	-1.06	4.43	2	9	0.21	0.93
1H-4, 112	5.63	20.28	-1.35	3.37	0	1	0	0.1
1H-4, 120	5.71	20.36			0	0	0	0
1H-4, 130	5.81	20.46			0	0	0	0
1H-4, 140	5.91	20.56			0	0	0	0
1H-5, 1	6.02	20.67			1	1	0.15	0.15
1H-5, 10	6.11	20.76			0	0	0	0
1H-5, 20	6.21	20.86			0	0	0	0
1H-5, 32	6.33	20.98			0	0	0	0
1H-5, 39	6.40	21.05			0	0	0	0
1H-5, 50	6.51	21.16			0	0	0	0
1H-5, 60	6.61	21.26			0	0	0	0
1H-5, 70	6.71	21.36			0	0	0	0
1H-5, 80	6.81	21.46			0	0	0	0
1H-5, 90	6.91	21.56			0	0	0	0
1H-5, 100	7.01	21.66			0	0	0	0
1H-5, 111	7.12	21.77	-0.90	3.42	6	3	0.85	0.42
1H-5, 120	7.21	21.86	-0.70	3.14	11	3	1.48	0.4
1H-5, 130	7.31	21.96	-0.61	3.19	14	1	1.79	0.13
1H-5, 140	7.41	22.06			2	0	0.2	0
1H-6, 1	7.52	22.17			16	0	1.71	0
1H-6, 11	7.62	22.27	-0.84	3.42	16	7	1.33	0.58
1H-6, 22	7.73	22.38	-0.87	3.86	11	17	1.09	1.68
1H-6, 30	7.81	22.46	-1.06	4.24	13	21	1.88	3.04
1H-6, 40	7.91	22.56	-1.03	4.74	5	6	0.81	0.97
1H-6, 50	8.01	22.66	-1.32	4.81	0	3	0	0.33
1H-6, 63	8.14	22.79	-1.17	4.32	1	2	0.1	0.2
1H-6, 70	8.21	22.86	-1.05	4.96	0	7	0	0.73
1H-6, 81	8.32	22.97	-0.94	4.89	0	1	0	0.1
1H-6, 90	8.41	23.06			0	0	0	0
1H-6, 100	8.51	23.16			0	0	0	0
1H-6, 114	8.65	23.30	-1.21	4.45	0	4	0	0.7
1H-6, 122	8.73	23.38	-1.29	4.45	0	6	0	0.64
1H-6, 135	8.86	23.51	-1.06	4.41	0	39	0	5.65
1H-6, 143	8.94	23.59	-0.96	5.63	0	8	0	0.96
1H-6, 143	8.94	23.59	-1.07	4.44				
1H-7, 1	9.02	23.67			0	1	0	0.11
1H-7, 10	9.11	23.76	-1.29	4.42	2	35	0.27	4.79
1H-7, 22	9.23	23.88	-1.26	4.36	0	9	0	2.1
1H-7, 30	9.31	23.96	-1.19	4.37	0	10	0	2.04
<b>145-883B-</b>								
3H-4, 0	21.91	23.96	-1.46	4.40	2	25	0.26	3.22
3H-4, 10	22.01	24.06	-1.55	4.33	0	20	0	4.61
3H-4, 20	22.11	24.16	-1.15	4.35	0	21	0	5.38
3H-4, 30	22.21	24.26	-0.97	4.37	1	3	0.1	0.3
3H-4, 38	22.29	24.34			0	0	0	0
3H-4, 48	22.39	24.44			0	0	0	0
3H-4, 61	22.52	24.57	-1.00	4.30	0	11	0	2.32
3H-4, 68	22.59	24.64	-0.74	4.28	1	2	0.1	0.2
3H-4, 78	22.69	24.74			0	0	0	0
3H-4, 88	22.79	24.84			0	0	0	0
3H-4, 104	22.95	25.00			0	0	0	0
3H-4, 110	23.01	25.06			0	0	0	0
3H-4, 122	23.13	25.18	-0.72	3.82	1	9	0.14	1.23
3H-4, 128	23.19	25.24	-0.54	3.86	2	3	0.23	0.35
3H-4, 140	23.31	25.36			0	0	0	0
3H-5, 0	23.41	25.46	-0.88	3.65	1	2	0.15	0.3
3H-5, 10	23.51	25.56			1	1	0.13	0.13
3H-5, 20	23.61	25.66			0	2	0	0.24
3H-5, 30	23.71	25.76	-0.99	3.60	1	1	0.16	0.16
3H-5, 38	23.79	25.86			2	0	0.39	0
3H-5, 48	23.89	25.94	-0.29	3.60	1	3	0.15	0.45
3H-5, 63	24.04	26.09	3.41	12.07	3	5	0.44	0.73
3H-5, 73	24.14	26.19	-0.50	3.69	0	2	0	0.22
3H-5, 83	24.24	26.29	-0.56	3.58	6	8	0.8	1.07
3H-5, 92	24.33	26.38	-0.49	3.74	3	8	0.37	0.99
3H-5, 101	24.42	26.47	-0.44	3.90	2	9	0.23	1.04
3H-5, 110	24.51	26.56	-0.58	3.95	5	9	0.76	1.37

## APPENDIX (continued).

Core, section, interval (cm)	Depth (mbsf)	Composite		$\delta^{13}\text{C}$ <i>Uvig.</i>	$\delta^{18}\text{O}$ <i>Uvig.</i>	<i>Cibs.</i> ( <i>N</i> )	<i>Uvig.</i> ( <i>N</i> )	<i>Cibs.</i> (per gm)	<i>Uvig.</i> (per gm)
		depth (m)	<i>Uvig.</i>						
3H-5, 119	24.60	26.65	-0.46	4.06	5	16	0.77	2.47	
3H-5, 128	24.69	26.74	-0.46	4.16	3	15	0.43	2.17	
3H-5, 140	24.81	26.86	-0.38	4.07	4	12	0.64	1.93	
3H-6, 0	24.91	26.96	-0.48	3.96	9	12	1.06	1.41	
3H-6, 10	25.01	27.06	-0.55	3.92	3	5	0.32	0.53	
3H-6, 20	25.11	27.16	-0.77	4.11	2	5	0.19	0.48	
3H-6, 30	25.21	27.26	-0.86	4.00	3	6	0.3	0.61	
3H-6, 38	25.29	27.34	-1.10	4.02	3	11	0.33	1.21	
3H-6, 48	25.39	27.44	-0.86	4.15	4	22	0.4	2.19	
3H-6, 72	25.63	27.68	-0.91	4.37	1	7	0.1	0.7	
3H-6, 82	25.73	27.78	-0.94	4.45	2	22	0.24	2.66	
3H-6, 92	25.83	27.88	-1.12	4.34	15	16	1.88	2.01	
3H-6, 101	25.92	27.97	-0.98	4.35	3	40	0.42	5.58	
3H-6, 113	26.04	28.09	-0.84	4.42	2	2	0.2	0.2	
3H-6, 122	26.13	28.18	-1.05	4.40	1	8	0.13	1.05	
3H-6, 128	26.19	28.24	-1.00	4.41	1	9	0.11	1.03	
3H-6, 140	26.31	28.36			1	0	0.12	0	
3H-7, 0	26.41	28.46			0	0	0	0	
3H-7, 10	26.51	28.56	-0.90	4.05	0	11	0	1.26	
3H-7, 20	26.61	28.66	-0.80	4.01	0	13	0	1.49	
3H-7, 30	26.79	28.84	-2.84	3.80	0	1	0	0.1	
3H-7, 38	26.71	28.76	-1.16	3.75	3	58	0.34	6.52	
3H-7, 48	26.89	28.94	-1.12	4.30	0	1	0	0.11	
3H-7, 61	27.02	29.07	-0.91	3.77	9	9	1.04	1.04	
145-883C-									
2H-2, 122	5.72	7.27			0	0	0	0	
2H-2, 131	5.81	7.36			0	0	0	0	
2H-2, 140	5.90	7.45			0	0	0	0	
2H-3, 1	6.01	7.56	-0.92	4.00	190	17	21.59	1.93	
2H-3, 12	6.12	7.67	-1.06	4.54	24	4	3.31	0.55	
2H-3, 18	6.18	7.73	-1.04	4.44	44	4	5.94	0.54	
2H-3, 30	6.30	7.85	-1.04	4.76	52	4	8.14	0.63	
2H-3, 40	6.40	7.95	-1.28	4.86	44	4	7.11	0.65	
2H-3, 48	6.48	8.03	-1.15	5.08	9	0	1.28	0	
2H-3, 60	6.60	8.15	-1.45	4.85	23	3	3.27	0.43	
2H-3, 70	6.70	8.25	-1.14	4.79	13	5	1.49	0.57	
2H-3, 78	6.78	8.33	-1.20	4.48	2	0	0.27	0	
2H-3, 88	6.88	8.43	-0.87	4.93	4	4	0.54	0.54	
2H-3, 100	7.00	8.55			1	0	0.11	0	
2H-3, 106	7.06	8.61			0	0	0	0	
2H-3, 120	7.20	8.75			1	1	0.12	0.12	
2H-3, 130	7.30	8.85			0	0	0	0	
2H-3, 134	7.34	8.89			0	0	0	0	
145-883D-									
1H-1, 1	0.01	0.01	-0.48	3.32	38	4	9.85	1.04	
1H-1, 9	0.09	0.09	-0.97	4.12	15	4	3.51	0.94	
1H-1, 19	0.19	0.19	-0.81	3.47	10	2	2.46	0.49	
1H-1, 29	0.29	0.29	-0.88	3.98	17	2	3.73	0.44	
1H-1, 39	0.39	0.39	-0.78	4.03	37	1	9.93	0.27	
1H-1, 49	0.49	0.49	-1.18	4.14	13	1	5.08	0.39	
1H-1, 59	0.59	0.59	-0.89	4.52	11	2	4.1	0.75	
1H-1, 69	0.69	0.69	-0.76	4.75	16	1	5.15	0.32	
1H-1, 79	0.79	0.79	-0.82	4.67	42	0	12.84	0	
1H-1, 89	0.89	0.89	-0.94	4.90	34	0	9.5	0	
1H-1, 97	0.97	0.97	-0.94	5.13	36	3	9.21	0.77	
1H-1, 109	1.09	1.09	-0.79	4.97	20	2	4.83	0.48	
1H-1, 119	1.19	1.19	-0.82	4.98	14	5	3.71	1.33	
1H-1, 129	1.29	1.29	-0.70	5.05	17	3	4.94	0.87	
1H-1, 139	1.39	1.39	-0.83	4.98	12	3	3.32	0.83	
1H-2, 1	1.51	1.51	-0.78	4.87	14	2	4.09	0.58	
1H-2, 9	1.59	1.59	-0.70	4.78	8	3	2.17	0.81	
1H-2, 19	1.69	1.69	-0.66	4.77	9	7	2.26	1.76	
1H-2, 29	1.79	1.79	-0.78	4.83	4	0	1.05	0	
1H-2, 39	1.89	1.89	-0.59	4.74	2	0	0.54	0	
1H-2, 49	1.99	1.99	-0.56	4.83	4	1	1.05	0.26	
1H-2, 59	2.09	2.09	-0.84	4.58	5	5	1.31	1.31	
1H-2, 69	2.19	2.19	-0.92	4.40	8	2	2.3	0.57	
1H-2, 79	2.29	2.29	-0.74	4.40	9	1	2.14	0.24	
1H-2, 89	2.39	2.39	-0.43	4.52	2	2	0.52	0.52	
1H-2, 99	2.49	2.49	-0.85	4.47	7	4	1.71	0.98	
1H-2, 107	2.57				0	0	0	0	
1H-2, 119	2.69		-0.89	4.16	11	3	3.03	0.83	
1H-2, 129	2.79		-0.66	4.45	6	0	1.59	0	
1H-2, 139	2.89		-0.81	4.34	13	2	3.23	0.5	
1H-3, 1	3.01	3.01	-0.89	4.37	15	1	4.75	0.32	
1H-3, 9	3.09	3.09	-0.91	4.50	18	2	4.83	0.54	
1H-3, 19	3.19	3.19	-1.15	4.29	10	0	2.29	0	
1H-3, 29	3.29	3.29	-1.29	4.23	7	0	1.98	0	
1H-3, 39	3.39	3.39	-0.92	4.34	8	0	2.02	0	
1H-3, 49	3.49	3.49	-0.84	4.44	3	0	0.79	0	
1H-3, 59	3.59	3.59	-1.28	4.32	30	2	9.52	0.63	
1H-3, 69	3.69	3.69			0	1	0	0.22	
1H-3, 79	3.79	3.79	-0.77	4.69	2	0	0.48	0	
1H-3, 89	3.89	3.89			0	0	0	0	
1H-3, 99	3.99	3.99			0	0	0	0	
1H-3, 109	4.09	4.09	-1.05	4.24	4	0	1.32	0	
1H-3, 119	4.19	4.19	-0.90	4.17	16	0	5.3	0	
1H-3, 129	4.29	4.29			0	0	0	0	
1H-3, 139	4.39	4.39			0	0	0	0	

## APPENDIX (continued).

Core, section, interval (cm)	Depth (mbsf)	Composite depth (m)	$\delta^{13}\text{C}$ <i>Uvig.</i>	$\delta^{18}\text{O}$ <i>Uvig.</i>	<i>Cibs.</i> (N)	<i>Uvig.</i> (N)	<i>Cibs.</i> (per gm)	<i>Uvig.</i> (per gm)
1H-4, 1	4.51	4.51	-0.96	4.07	14	0	4.57	0
1H-4, 9	4.59	4.59	-1.20	3.93	1	0	0.27	0
1H-4, 19	4.69	4.69			0	0	0	0
1H-4, 29	4.79	4.79	-1.06	3.49	3	0	0.83	0
1H-4, 39	4.89	4.89	-0.85	3.74	35	1	9.79	0.28
1H-4, 49	4.99	4.99	-1.04	3.29	33	2	9.14	0.55
1H-4, 49	4.99	4.99	-0.74	3.75				
1H-4, 59	5.09	5.09			0	0	0	0
1H-4, 69	5.19	5.19			0	0	0	0
1H-4, 79	5.29	5.29			0	0	0	0
1H-4, 89	5.39	5.39			0	0	0	0
1H-4, 99	5.49	5.49			0	0	0	0
1H-4, 109	5.59	5.59			0	0	0	0
1H-4, 119	5.69	5.69			0	0	0	0
1H-4, 129	5.79	5.79			0	0	0	0
1H-4, 139	5.89	5.89			0	0	0	0
1H-5, 1	6.01	6.01			0	0	0	0
1H-5, 9	6.09	6.09			0	0	0	0
1H-5, 19	6.19	6.19			0	0	0	0
1H-5, 29	6.29	6.29			0	1	0	0.22
1H-5, 39	6.39	6.39			0	0	0	0
1H-5, 49	6.49	6.49			0	0	0	0
1H-5, 59	6.59	6.59			0	0	0	0
1H-5, 69	6.69	6.69			0	0	0	0
1H-5, 79	6.79	6.79			0	0	0	0
1H-5, 89	6.89	6.89			0	0	0	0
1H-5, 99	6.99	6.99			0	0	0	0
1H-5, 109	7.09	7.09			0	1	0	0.28
1H-5, 119	7.19	7.19			2	4	0.49	0.98
1H-5, 129	7.29	7.29	-0.77	3.33	6	1	1.24	0.21
1H-cc, 1	7.40	7.40	-1.02	3.91	42	1	10.49	0.25
2H-1, 2	7.52	9.02	-1.14	4.78	1	0	0.15	0
2H-1, 20	7.70	9.20	-1.28	4.64	32	1	4.3	0.13
2H-1, 30	7.80	9.30	-1.32	4.61	14	4	1.75	0.5
2H-1, 40	7.90	9.40	-1.34	4.32	73	4	8.56	0.47
2H-1, 50	8.00	9.50	-1.46	4.27	11	0	1.16	0
2H-1, 60	8.10	9.60	-1.39	4.34	6	2	0.66	0.22
2H-1, 70	8.20	9.70			0	0	0	0
2H-1, 80	8.30	9.80			0	1	0	0.1
2H-1, 90	8.40	9.90			0	0	0	0
2H-1, 100	8.50	10.00	-1.42	4.66	22	0	2.65	0
2H-1, 110	8.60	10.10	-1.29	4.23	33	0	3.71	0
2H-1, 120	8.70	10.20	-1.27	4.36	2	0	0.21	0
2H-1, 130	8.80	10.30	-1.33	4.31	10	0	1.04	0
2H-1, 140	8.90	10.40	-1.23	4.39	3	0	0.32	0
2H-2, 1	9.01	10.51			0	0	0	0
2H-2, 10	9.10	10.60			0	0	0	0
2H-2, 20	9.20	10.70			0	0	0	0
2H-2, 30	9.30	10.80			0	0	0	0
2H-2, 40	9.40	10.90			0	0	0	0
2H-2, 50	9.50	11.00			0	0	0	0
2H-2, 60	9.60	11.10			0	0	0	0
2H-2, 70	9.70	11.20			0	0	0	0
2H-2, 82	9.82	11.32			0	0	0	0
2H-2, 90	9.90	11.40			0	0	0	0
2H-2, 100	10.00	11.50			0	0	0	0
2H-2, 110	10.10	11.60			0	0	0	0
2H-2, 120	10.20	11.70			0	0	0	0
2H-2, 130	10.30	11.80			0	0	0	0
2H-2, 140	10.40	11.90			0	0	0	0
2H-3, 1	10.51	12.01	-0.63	3.51	1	1	0.12	0.12
2H-3, 10	10.60	12.10			0	0	0	0
2H-3, 20	10.70	12.20			1	1	0.11	0.11
2H-3, 40	10.90	12.40			0	0	0	0
2H-3, 50	11.00	12.50			0	0	0	0
2H-3, 60	11.10	12.60			0	0	0	0
2H-3, 70	11.20	12.70			0	0	0	0
2H-3, 79	11.29	12.79	-1.13	4.15	1	0	0.09	0
2H-3, 90	11.40	12.90			0	0	0	0
2H-3, 100	11.50	13.00			1	0	0.16	0
2H-3, 110	11.60	13.10			0	0	0	0
2H-3, 120	11.70	13.20			0	0	0	0
2H-3, 130	11.80	13.30			0	0	0	0
2H-3, 140	11.90	13.40			0	0	0	0
2H-4, 1	12.01	13.51			0	0	0	0
2H-4, 10	12.10	13.60			0	0	0	0
2H-4, 20	12.20	13.70	-1.25	4.02	17	2	2.55	0.3
2H-4, 30	12.30	13.80	-0.91	3.84	36	6	4.1	0.68
2H-4, 70	12.70	14.20	-1.26	3.31	13	2	4.91	0.75
2H-4, 70	12.70	14.20	-1.09	3.55				
2H-4, 80	12.80	14.30	-1.08	3.75	18	3	6.27	1.05
2H-4, 90	12.90	14.40			0	1	0	0.37
2H-4, 100	13.00	14.50			0	5	0	0.8
2H-4, 110	13.10	14.60	-1.56	4.28	4	3	0.52	0.39
2H-4, 120	13.20	14.70	-1.43	4.44	4	3	0.47	0.35
2H-4, 130	13.30	14.80	-1.66	4.34	2	4	0.24	0.48
2H-4, 140	13.40	14.90			1	3	0.11	0.32
2H-5, 1	13.51	15.01	-1.58	4.45	5	8	0.7	1.12
2H-5, 10	13.60	15.10	-1.58	4.24	23	9	2.72	1.06
2H-5, 20	13.70	15.20			1	3	0.1	0.3

## APPENDIX (continued).

Core, section, interval (cm)	Depth (mbsf)	Composite		$\delta^{13}\text{C}$ <i>Uvig.</i>	$\delta^{18}\text{O}$ <i>Uvig.</i>	<i>Cibs.</i> ( <i>N</i> )	<i>Uvig.</i> ( <i>N</i> )	<i>Cibs.</i> (per gm)	<i>Uvig.</i> (per gm)
		depth (m)	<i>Uvig.</i>						
2H-5, 30	13.80	15.30				1	5	0.11	0.57
2H-5, 40	13.90	15.40				0	0	0	0
2H-5, 50	14.00	15.50				0	1	0	0.1
2H-5, 60	14.10	15.60				0	0	0	0
2H-5, 70	14.20	15.70				0	2	0	0.2
2H-5, 80	14.30	15.80				0	0	0	0
2H-5, 90	14.40	15.90				0	0	0	0
2H-5, 100	14.50	16.00	-0.87	4.42		3	0	0.27	0
2H-5, 110	14.60	16.10				0	0	0	0
2H-5, 130	14.80	16.30				0	0	0	0
2H-5, 140	14.90	16.40	-0.98	4.28		7	0	1.38	0
2H-6, 1	15.01	16.51				0	0	0	0
2H-6, 10	15.10	16.60				0	0	0	0
2H-6, 20	15.20	16.70	-1.60	3.26		2	0	0.24	0
2H-6, 30	15.30	16.80	-1.02	3.77		3	2	0.33	0.22
2H-6, 40	15.40	16.90	-1.12	3.82		10	0	0.94	0
2H-6, 60	15.60	17.10				0	0	0	0
2H-6, 70	15.70	17.20				0	0	0	0
2H-6, 80	15.80	17.30	-1.63	4.00		9	0	1.45	0
2H-6, 90	15.90	17.40	-1.10	4.04		3	2	0.31	0.21
2H-6, 100	16.00	17.50				0	0	0	0
2H-6, 110	16.10	17.60				0	0	0	0
2H-6, 120	16.20	17.70				0	0	0	0
2H-6, 130	16.30	17.80				0	0	0	0
2H-6, 140	16.40	17.90				0	0	0	0
2H-7, 1	16.51	18.01				0	0	0	0
2H-7, 10	16.60	18.10				0	0	0	0
2H-7, 20	16.70	18.20				0	0	0	0
2H-7, 30	16.80	18.30				0	0	0	0
2H-7, 40	16.90	18.40	-1.03	3.20		5	4	0.62	0.5
2H-7, 50	17.00	18.50	-0.78	3.03		3	4	0.31	0.42
2H-cc, 1	17.18	18.68	-0.90	3.33		1	0	0.07	0

Note: *Uvig.* = *Uvigerina*, and *Cibs.* = *Cibicidoides*.